

Photocatalytic Activity of Iron-Doped Titania Coupled with Biochar for Wastewater Treatment

Domenico Rosa^{a,*}, Nigar Abbasova^b, Martina Fazi^a

^aDipartimento di Ingegneria Chimica Materiali Ambiente, Sapienza-Università di Roma, Via Eudossiana 18, 00184 Roma, Italia

^bDepartment of Ecology, Azerbaijan University of Architecture and Construction, Baku, Azerbaijan
domenico.rosa@uniroma1.it

The photocatalytic activity of iron-doped titania nanoparticles under visible light was enhanced through coupling with biochar. Preliminary tests evaluated the adsorption capacities of biochar derived from various sources, including coffee grounds, mate wood, deglet noir date pits, and licorice roots. Based on these results, different synthesis strategies were explored to select the most effective catalyst for degrading methylene blue, paracetamol, and methyl orange, which represent cationic, neutral, and anionic contaminants, respectively. The most effective catalyst was identified as an iron-doped nano-titania coupled with licorice-derived biochar, produced via an innovative solid-state synthesis method that is both waste-free and efficient. This composite catalyst performance was compared with a similar catalyst lacking biochar. Among the biochar sources tested, licorice biochar demonstrated the highest adsorption capacity and significantly enhanced the photocatalytic activity of the iron-doped titania. Results indicated that the composite catalyst was most effective in degrading cationic contaminants, while its efficiency for neutral and anionic molecules was comparatively lower.

1. Introduction

The increasing presence of emerging pollutants in wastewater poses a challenge for conventional treatment systems, which often fail to remove them effectively, which are harmful even at low concentrations. In this context, photocatalysis has emerged as a promising technology for degrading such contaminants, utilizing a light-activated catalyst to generate reactive species capable of oxidizing pollutants.

The most widely used photocatalyst is titanium dioxide (titania, TiO₂), due to its chemical stability, non-toxicity, and high oxidative potential (Tahir et al., 2023). However, its wide band gap (~3.2 eV) restricts activity to UV radiation, constituting only a small fraction of sunlight. To overcome this limitation, doping is employed, introducing foreign elements (like Fe, Cd, N) into the TiO₂ crystal structure to reduce the band gap and enable activation under visible light.

Despite doping improving light absorption, pollutant removal kinetics often remain low. To enhance photocatalytic efficiency, many studies have explored coupling TiO₂ with other materials, including biochar (Garcia et al., 2021; Leary & Westwood, 2011; Silva et al., 2021). Biochar is a carbonaceous material obtained from the pyrolysis of plant residues, characterized by high porosity and adsorptive capacity. Its use enhances photocatalytic performance and promotes a circular economy by valorizing organic waste.

The integration of biochar with photocatalysis offers several advantages: (i) Formation of heterojunctions, which improve charge separation and reduce electron-hole recombination, (ii) Increased specific surface area, which enhances pollutant adsorption and facilitates subsequent photocatalytic degradation, (iii) Improved stability and reusability of the catalyst, thanks to the porous structure and chemical resistance of biochar.

This study aims to develop and characterize various TiO₂-based catalysts coupled with biochar derived from plant residues. The synthesized materials were tested on different model contaminants to assess system effectiveness and determine the optimal combination for emerging pollutant removal.

2. Materials and method

2.1 Biochar synthesis

Four different waste materials were used as biochar precursors: Arabica blend coffee grounds (CG), waste wood from yerba-mate processing (MW), Deglet Nour date seeds (DN), and root licorice processing waste (LR) provided by Amarelli SRL. Only physical preliminary treatments were applied: all waste materials were washed with demineralized water and dried in an oven at 40 °C for 24 hours. Subsequently, they were ground into a fine powder, except for licorice, which retained its characteristic filamentous structure even after grinding. The ground materials were further washed with demineralized water, filtered, and dried again at 40 °C for 24 hours to obtain an anhydrous product. Each pretreated waste material was placed in an autoclave and subsequently subjected to pyrolysis in a furnace at 700 °C for 2 hours (Rosa et al., 2024). The resulting materials were labeled as BC, with a subscript indicating the initial feedstock. For example, biochar derived from licorice root was designated as BC_{LR}.

2.2 Titania synthesis

Titania was synthesized using titanium diisopropoxide bis(acetylacetonate) (75 wt.% in isopropanol, Alfa Aesar) as the precursor. Specifically, 10.5 mL of the precursor was dissolved in 30 mL of absolute ethanol (>99.8%, Honeywell) and added dropwise to 60 mL of demineralized water (16 $\mu\text{S}/\text{cm}^2$) at 80 °C under continuous stirring. The reaction mixture was stirred for 4 hours. The resulting solid was recovered through multiple centrifugation steps, washed with distilled water, dried at 60 °C overnight, ground into a fine powder, and subsequently calcined at 500 °C for 2 hours.

2.3 Titania doping/composite material synthesis

Titania doping with iron (1%Fe-TiO₂) was performed via a solid-state method (Rosa et al., 2023). The role of the Fe is helpful to band gap narrowing, thereby extending the photocatalytic activity of TiO₂ into the visible light region. Additionally, four different syntheses were explored to produce composite materials: material "A" was synthesized following a literature-reported method (Silva et al., 2021), while materials "B" and "C" were obtained using a novel approach starting from different precursors. Material "D" was synthesized through an additional novel procedure, as described below.

Solid-State Doping with Iron (1% Fe-TiO₂): Titania was doped with iron using a solid-state method. Specifically, synthesized TiO₂ was ground in a mortar with hexahydrated ferric chloride (FeCl₃·6H₂O, Honeywell) at a 1 wt% ratio relative to titania, as previous study (Rosa et al., 2023) identified this as the optimal concentration (0.500 g TiO₂ and 0.024 g FeCl₃·6H₂O). The homogeneous solid was then calcined at 600 °C for 3 hours.

Synthesis of Composite Material A: The composite material was synthesized in two steps, following a method reported in the literature (Silva et al., 2021): first, biochar was magnetized, followed by the in situ synthesis of titania on the magnetized biochar.

- **Magnetization Step:** Magnetic nanoparticles were prepared via coprecipitation. Fe²⁺ and Fe³⁺ salts (FeCl₃·6H₂O:FeSO₄·7H₂O, 1:3 w/w) were dissolved in 50 mL of distilled water, and biochar (BC) was added at a mass ratio of 1:6 (w/w) relative to the iron salt content. A 0.5 mol/L KOH solution (50 mL) was then added dropwise. The mixture was maintained at 75 °C under constant stirring for 1 hour. The resulting black precipitate (magBC) was magnetically separated, washed with distilled water until neutral pH, and dried at 40 °C overnight.
- **Final Synthesis Step:** The magBC/TiO₂ heterostructure was obtained via solvothermal synthesis. In the first step, 58 mg of magBC was suspended in 45 mL of ethanol for 5 minutes at room temperature (Solution A). Solution B was prepared by adding 1 mL of titanium diisopropoxide bis(acetylacetonate) (75 wt% in isopropanol) to 15 mL of ethanol, followed by stirring for 5 minutes. Solution B was then added dropwise under continuous stirring to Solution A. A third solution, containing 3 mL of demineralized water and 15 mL of ethanol, was then added dropwise to the mixture, which was stirred for an additional 5 minutes. The final mixture was transferred to a Teflon-lined stainless-steel autoclave and heated at 160 °C for 3 hours. After cooling, the suspension was centrifuged at 5500 rpm for 10 minutes. The recovered solid was washed three times with water and ethanol and finally dried at 60 °C overnight (Silva et al., 2021).

Materials B and C were synthesized using a solid-state approach by grinding BC with 1%Fe-TiO₂ for material B, and magnetized biochar (magBC) with 1%Fe-TiO₂ for material C. The BC/Ti ratio was maintained equal to that of material A. Specifically, 58 mg of BC (or magBC) was mixed with 230 mg of 1%Fe-TiO₂ (corresponding to an 80% Ti-20% BC/magBC ratio). The mixture was then transferred to an autoclave and heated at 160 °C for 3 hours.

Material D was synthesized via a solid-state approach by grinding pretreated waste biomass (raw, non-carbonized) with 1%Fe-TiO₂. The resulting mixture was then calcined at 700 °C for 2 hours. The samples, for heat treatment, were placed in a muffle furnace once the set point temperature was reached.

The biomass-to-TiO₂ ratio was set to maintain consistency with materials A, B, and C. Specifically, 232 mg of biomass (four times the amount used in other syntheses, i.e., 58 mg, considering a yield of biochar of 25%) was mixed with 230 mg of 1%Fe-TiO₂.

All samples were then stored at room temperature in closed vials.

2.4 Evaluation of contaminant removal properties

Preliminary adsorption batch tests were carried to assess the efficiency of biochars in removing methylene blue (MB, C₁₆H₁₈N₃SCl·3H₂O, Sigma Aldrich), paracetamol (PC, C₈H₉NO₂, Carlo Erba), and methyl orange (MO, C₁₄H₁₄N₃NaO₃S, Carlo Erba) from solution, each at an initial concentration of 10 mg/L. The most effective biochar was identified based on its adsorption capacity at equilibrium, which was verified by monitoring the stabilization of removal over time. Equilibrium was considered reached when no further increase in adsorption was observed, which occurred after 28 hours. After this period, samples were filtered through 2–3 µm filter paper.

Batch experiments were carried out in glass beakers containing 20 mL of contaminant solution, using a BC dosage of 1 g/L. The suspensions were stirred at 350 rpm with a magnetic stirrer for 28 h. At the end of the process, the supernatant was analyzed via UV-Vis spectrophotometry (PG Instruments T80+).

The contaminant removal efficiency (η) was calculated using Equation (1):

$$\eta = \frac{A_0 - A_t}{A_0} \cdot 100 \quad (1)$$

where η represents the removal efficiency (%), A_0 is the initial absorbance of the reference solution, and A_t is the absorbance of the sample at time t . The absorbance values considered corresponded to the maximum peak of each contaminant.

Photocatalytic activity tests were carried out following the same procedure, with an additional step to allow contaminant adsorption on the catalyst surface. Specifically, samples were pre-treated in the dark for 30 minutes before exposure to visible light, provided by a 13 W LED lamp (irradiance: 41 W/m²). Control experiments were performed in the dark to assess the intrinsic adsorptive capacity of the nanoparticles and to quantify the enhancement in contaminant removal upon catalyst activation under visible light.

3. Results and discussion

3.1 Biochar adsorption capacity

Adsorption test results are shown in Table 1.

Table 1: Adsorbent capacity (mg/g) at equilibrium adsorption of various biochar for different adsorbates.

Adsorbate	CG	MW	DN	LR
MB	9.5	22.2	23.0	75.1
PC	21.5	65.4	64.1	136.9
MO	0.6	0.1	0.2	0.5

The adsorption results revealed significant differences in the capacity of biochars derived from various precursors to remove MB, PC, and MO from aqueous solutions.

MB exhibited relatively high adsorption capacity across all adsorbents, with a value of 9.5 mg/g for the biochar derived from CG. This capacity increased considerably for biochar obtained from MW and DN, reaching 22.2 mg/g and 23.0 mg/g, respectively. However, the highest adsorption was observed with biochar produced by LR, which reached 75.1 mg/g. This result suggested that LR possessed favorable physicochemical characteristics for MB adsorption, likely due to its high specific surface area, functional groups capable of interacting with the cationic dye, and a microporous structure suitable for accommodating MB molecules.

The adsorption behavior of PC followed a similar trend, although with generally higher adsorption values. For the biochar derived from CG, the adsorption capacity was 21.5 mg/g, more than twice that of MB. As observed for MB, PC adsorption increased significantly with the use of biochar from MW and DN, which exhibited comparable values (65.4 mg/g and 64.1 mg/g, respectively). However, the biochar derived from LR again showed the highest adsorption capacity, reaching 136.9 mg/g. This strong affinity could be due to PC's ability to form specific interactions with the adsorbent surface, such as hydrogen bonding or π - π interactions, which were likely enhanced by the chemical composition and porosity of BC_{LR}.

Conversely, MO exhibited a markedly different behavior compared to MB and PC, with extremely low adsorption values across all adsorbents. Adsorption on MW and DN was almost negligible (0.1-0.2 mg/g), and the other biochars also demonstrated very limited retention, with a maximum of only 0.6 mg/g for the BC_{CG}. This poor affinity suggested weak or unfavorable interactions between MO and the tested biochars. A possible explanation lies in the anionic nature of MO, which likely reduced its adsorption on biochar due to its predominantly negative surface charge at neutral pH, leading to electrostatic repulsion and hindering MO adsorption.

It is noteworthy that while BC_{CG} exhibited the lowest adsorption performance for MB and PC, it demonstrated the highest, albeit limited, adsorption capacity for MO among all the tested biochars. This behavior can be due to the acidic nature of CG biomass, which predominantly contains positively charged surface functional groups, enhancing its effectiveness in anion removal (Al-Awadhi et al., 2022). Consequently, BC_{CG} exhibited the lowest affinity for MB, a cationic dye.

Overall, biochar derived from LR was the most effective in adsorbing both MB and PC, whereas biochar from CG exhibited the lowest adsorption capacity among the tested materials. The highly selective behavior of MO suggested that adsorption efficiency depended not only on the nature of the biochar but also on the physicochemical properties of the adsorbates, particularly charge, polarity, and molecular size.

Due to their superior adsorption performance, the most effective materials (DN and LR) were selected for subsequent coupling experiments with titania.

3.2 Photocatalytic properties

To evaluate the removal efficiency and photocatalytic properties of composite materials A, B, C, and D, experiments were carried out under both dark (only adsorption) and visible light conditions for 3 hours, with an irradiance of 41 W/m² and an initial MB concentration of 10 mg/L. Irradiance has an important role in photocatalytic processes, as it directly affects the production rate of electron-hole pairs and, consequently, the formation of reactive oxygen species. The selected irradiance value, provided by a low-cost commercial LED lamp, ensured effective activation of the photocatalyst under visible light without introducing excessive energy input that could lead to non-linear effects, such as electron-hole recombination, surface saturation, or overheating of the sample, which instead remained at room temperature. Although irradiance was not varied in this study, it is well known that changes in this parameter can significantly affect photocatalytic efficiency.

For comparison, the same tests were also performed on TiO₂ and 1%Fe-TiO₂. Additionally, materials DN and LR, which exhibited the highest adsorption performance, were further tested, and the results are presented in Figure 1a-b.

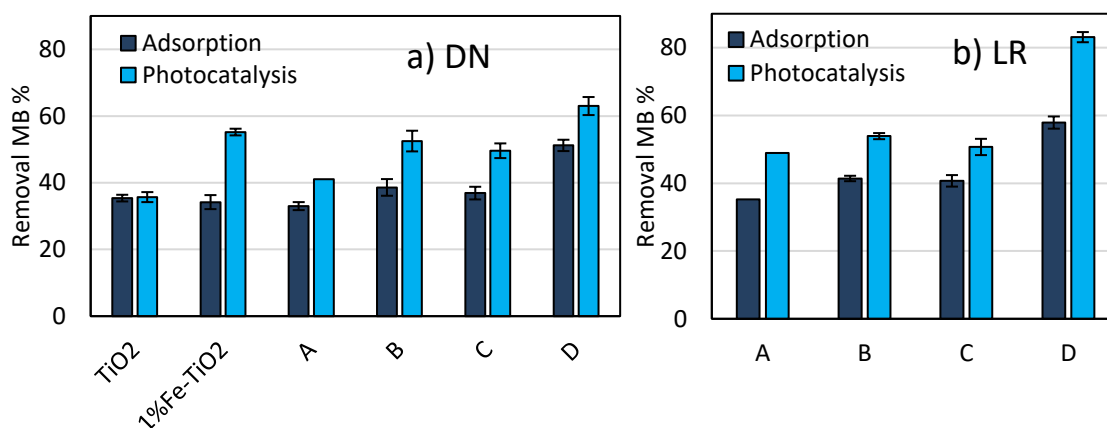


Figure 1: MB removal % comparison using different materials. Conditions: temperature 25 °C, pH neutral, treatment time 3 h, initial concentration 10 mg/L MB, Irradiance 41 W/m². Biomass used for composites: a) DN and b) LR.

No photocatalytic activity under visible light was observed for pure titania, whereas all other tested materials exhibited significant activity under visible radiation. This enhanced performance can be due to the synergistic effect between biochar and titania (Briche et al., 2020). Due to its porous structure, biochar effectively adsorbs organic contaminants, bringing them into proximity with the titania surface and facilitating degradation via radical attack while mitigating mass transport limitations (Yu et al., 2020).

As a result, in all adsorption-only tests (performed in the absence of light), contaminant removal was higher for biochar-based composites, except for material A, which showed reduced adsorptive capacity compared to the 1%Fe-TiO₂ sample, demonstrating that the incorporation of biochar enhanced adsorption performance. The highest removal efficiency was achieved with composite D, synthesized from both DN and LR, the two materials that exhibited the best adsorption properties.

Moreover, since all tested materials exhibited photocatalytic activity, biochar proved to be an effective sensitizer for visible-light-driven titania, likely due to its strong light-absorbing properties (Rangarajan et al., 2022).

Across all experiments, composites containing LR outperformed those synthesized with DN, aligning with the adsorption data reported earlier. High removal efficiencies were also observed for 1%Fe-TiO₂ and material B, prompting further investigation of these materials. Additional tests were carried out using MB, PC and MO contaminants at an initial concentration of 10 mg/L, to evaluate removal % under visible light after 3 hours (Figure 2).

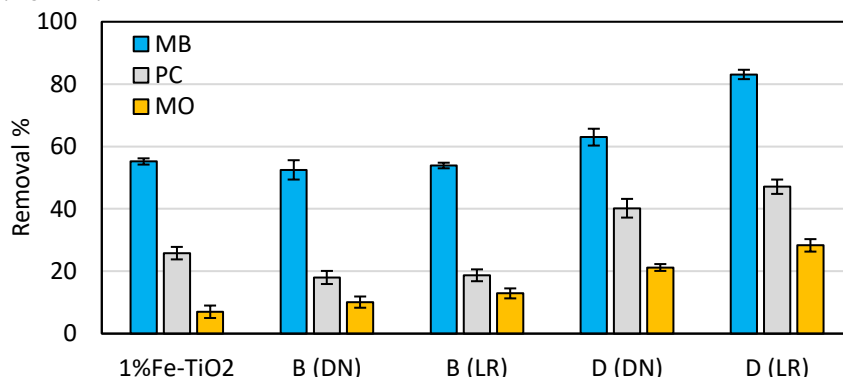


Figure 2: Comparison of MB, PC and MO removal % with different materials. Conditions: temperature 25 °C, pH neutral, treatment time 3 h, initial concentration 10 mg/L, Irradiance 41 W/m².

The results in Figure 2 confirmed that composites derived from licorice processing waste exhibited superior removal performance compared to those synthesized from DN. Consistent with previous experiments (Figure 1), composite D demonstrated the highest removal efficiency for MB, PC, and MO. However, while MO exhibited the lowest removal efficiency among the three contaminants, consistent with the adsorption tests reported in Table 1, the removal of PC was consistently lower than MB. This trend contrasts with the adsorption experiments using biochar, where PC was the most effectively adsorbed contaminant. This discrepancy could be due to the nature of the matrix, which influences the affinity between the adsorbent and the adsorbate.

In particular, paracetamol may have a stronger affinity for the aromatic domains of biochar, forming π - π interactions. These interactions are less prominent when the adsorbent is a titanium oxide matrix, which, in contrast, exhibited a greater affinity for methylene blue. This difference might be related to the chemical nature of the interactions involved. While PC interacts preferentially with carbonaceous materials through π - π stacking, MB, being a cationic dye, could interact more favorably with the surface hydroxyl groups and charge distribution of titania, possibly through electrostatic attraction.

Since adsorption and photocatalysis are closely interconnected processes, any reduction in adsorption negatively impacts photocatalytic efficiency. Hydroxyl radicals, which are photogenerated during the reaction, can only degrade molecules close to the photocatalyst surface due to their short half-life (Yu et al., 2020). Therefore, lower adsorption limits the availability of contaminants for photocatalytic degradation, ultimately reducing overall performance.

4. Conclusions

Various biochars and different synthesis methods for biochar-titania composite photocatalysts were tested. Among the biochars evaluated, the material derived from licorice roots demonstrated the highest adsorption capacity, effectively removing all three tested contaminants, MO, MB, and PC, to a greater extent than the other biochars. In all tested biochars, PC exhibited the highest adsorption, followed by MB, whereas MO was barely adsorbed.

Regarding the different coupling strategies, method D proved to be the most effective. This approach not only enabled the efficient valorization of an agro-industrial waste but was also simple to perform, based on a solid-state process that did not produce additional waste. Consistent with the adsorption tests, all composite materials exhibited photocatalytic activity under visible light, with those incorporating licorice root biochar showing

enhanced adsorption capacity and, consequently, improved photocatalytic performance compared to iron-doped titania.

Interestingly, while MO remained poorly removed even in the photocatalytic tests, consistent with its low adsorption affinity, an inversion in the removal trend of MB and PC was observed. Unlike the adsorption experiments, where PC was retained more effectively than MB, in the photocatalytic process, MB was removed to a greater extent than PC. This different behavior might be due to the stronger affinity of PC for carbonaceous matrices, whereas MB interacted more effectively with the metal oxide component.

Overall, the incorporation of biochar significantly enhanced the photocatalytic activity of the material. Moreover, the selected synthesis method proved to be simple, sustainable, and waste-free, offering a promising route for the development of efficient biochar–titania composites and the valorization of agro-industrial waste in line with circular economy principles. Looking ahead, future work could focus on reusability tests and evaluations using real wastewater, to assess the material's performance under more realistic conditions and explore its practical applicability.

References

- Al-Awadhi, Y. M., Pradhan, S., McKay, G., Al-Ansari, T., & Mackey, H. R. (2022). Coffee Waste Biochar: A Widely Available and Low-cost Biomass for Producing Carbonaceous Water Treatment Adsorbents. *Chemical Engineering Transactions*, 92, 319–324. <https://doi.org/10.3303/CET2292054>
- Briche, S., Derqaoui, M., Belaiche, M., El Mouchtari, E. M., Wong-Wah-Chung, P., & Rafqah, S. (2020). Nanocomposite material from TiO₂ and activated carbon for the removal of pharmaceutical product sulfamethazine by combined adsorption/photocatalysis in aqueous media. *Environmental Science and Pollution Research*, 27(20), 25523–25534. <https://doi.org/10.1007/s11356-020-08939-2>
- Garcia, R. M., Carleer, R., Pérez, M. A., Torres, J. P., Gu, Y., Samyn, P., & Yperman, J. (2021). Fe-TiO₂/AC and Co-TiO₂/AC composites: Novel photocatalysts prepared from waste streams for the efficient removal and photocatalytic degradation of cibacron yellow F-4G dye. *Catalysts*, 11(10). <https://doi.org/10.3390/catal11101137>
- Leary, R., & Westwood, A. (2011). Carbonaceous nanomaterials for the enhancement of TiO₂ photocatalysis. In *Carbon* (Vol. 49, Issue 3, pp. 741–772). <https://doi.org/10.1016/j.carbon.2010.10.010>
- Rangarajan, G., Jayaseelan, A., & Farnood, R. (2022). Photocatalytic reactive oxygen species generation and their mechanisms of action in pollutant removal with biochar supported photocatalysts: A review. In *Journal of Cleaner Production* (Vol. 346). Elsevier Ltd. <https://doi.org/10.1016/j.jclepro.2022.131155>
- Rosa, D., D'Agostino, F., Bavasso, I., & Di Palma, L., (2023). An Innovative and Easy Method for Iron-doped Titania Synthesis. *Chemical Engineering Transactions*, 101. <https://doi.org/10.3303/CET23101003>
- Rosa, D., Petruccelli, V., Iacoppi, M. C., Brasili, E., Badiali, C., Pasqua, G., & Di Palma, L. (2024). Functionalized biochar from waste as a slow-release nutrient source: Application on tomato plants. *Heliyon*, 10(8), e29455. <https://doi.org/10.1016/j.heliyon.2024.e29455>
- Silva, C. P., Pereira, D., Calisto, V., Martins, M. A., Otero, M., Esteves, V. I., & Lima, D. L. D. (2021). Biochar-TiO₂ magnetic nanocomposites for photocatalytic solar-driven removal of antibiotics from aquaculture effluents. *Journal of Environmental Management*, 294. <https://doi.org/10.1016/j.jenvman.2021.112937>
- Tahir, M., Alesayi, M. T., & Zahmi, S. Al. (2023). Fabricating Carbon Fibers (CFs)/TiO₂ Composite for Photocatalytic Green Hydrogen Production. *Chemical Engineering Transactions*, 106, 679–684. <https://doi.org/10.3303/CET23106114>
- Yu, M., Wang, J., Tang, L., Feng, C., Liu, H., Zhang, H., Peng, B., Chen, Z., & Xie, Q. (2020). Intimate coupling of photocatalysis and biodegradation for wastewater treatment: Mechanisms, recent advances and environmental applications. In *Water Research* (Vol. 175). Elsevier Ltd. <https://doi.org/10.1016/j.watres.2020.115673>